Available online at www.sciencedirect.com
SCIENCE DIRECT®
Journal of Nuclear Materials 319 (2003) 24–30
journal of nuclear materials
www.elsevier.com/locate/jnucmat

Reaction of yttria-stabilized zirconia with zirconium, silicon and Zircaloy-4 at high temperature: a compatibility study for cermet fuels

T. Arima *, T. Tateyama, K. Idemitsu, Y. Inagaki

Faculty of Engineering, Institute of Environmental Systems, Kyushu University, 6-10-1 Hakozaki, Fukuoka 812-8581, Japan

Abstract

Compatibility studies for cermet (ceramic and metal) fuels have been completed for a temperature range of 1073–1423 K. A reaction between yttria-stabilized zirconia (YSZ), as a simulated fuel, and Zr, as a candidate for a metallic matrix, has been observed at temperatures $\geqslant 1273$ K, which means the formation of a metallic reaction layer at the interface between YSZ and Zr and the occurrence of metallic phases inside the YSZ. Similar results were observed for the YSZ–Zry4 (cladding) system. On the other hand, the degree of reaction was relatively large for the YSZ–Si (metallic matrix) system, and Si diffused into the YSZ. However, the maximum fuel center-line temperature can be predicted to be less than $\approx$1273 K for cermet fuels. Therefore, compatibility between the ceramic fuel and the metallic matrix should be good under normal reactor operational conditions. Furthermore, since the temperature of the fuel-cladding gap is lower, the cermet fuel and the cladding material are compatible.

1. Introduction

Zirconia-based inert matrix fuels are likely to be an attractive fuel candidate for burning, in light water reactors (LWR), excess plutonium from LWR as well as from nuclear weapons. An inert matrix fuel (IMF) material based on yttria-stabilized zirconia (YSZ), $Y_yZr_{1-y}O_{2-y/2}$ ($y \geqslant 0.15$), was proposed by PSI [1]. For such a zirconia, it is important to stabilize the cubic lattice structure for a wide temperature range. So, the proper amounts of Y_2O_3 and PuO_2 were added to ZrO_2.

Cubic YSZ has advantages such as high melting point, chemical stability, low neutron capture cross-section and stability under irradiation. In addition to Y_2O_3 as the stabilizer, Er_2O_3 must be added to act as a burnable poison. As a result, the composition of the cubic zirconia as the inert matrix fuel is $Er_xY_yPu_z$-$Zr_{1-x-y-z}O_{2-(x+y)/2}$.

However, there is the drawback that the oxide fuel consisting only of zirconia-based material has a relatively low thermal conductivity. Thermal conductivity of zirconia has been measured by many researchers [2–4]. Pure monoclinic zirconia has a thermal conductivity of $\approx$6 $W\,m^{-1}\,K^{-1}$ at room temperature, and its value decreases with temperature [2]. However, zirconia stabilized by Y_2O_3, Er_2O_3 and/or CeO_2 has a thermal conductivity of 2–3 $W\,m^{-1}\,K^{-1}$ [2–4], and these values are relatively low compared to UO_2, as shown in Table 1. In addition, the thermal conductivity of stabilized zirconia is almost independent of temperature. Therefore, in order to improve such a thermal property, two types of reliable materials have been investigated so far. These are cermet (ceramic–metal) and cercer (ceramic–ceramic) fuels. The present study is focused on cermet consisting of IMF particles embedded in a metallic matrix. By combining oxide and metal, cermet fuels have a good thermal conductivity. Fig. 1 shows the temperature distribution in several types of fuel [5].

* Corresponding author. Tel.: +81-92 642 3779; fax: +81-92 642 3800.
E-mail address: arimatne@mbox.nc.kyushu-u.ac.jp (T. Arima).

0022-3115/03/$ - see front matter © 2003 Elsevier Science B.V. All rights reserved.
doi:10.1016/S0022-3115(03)00129-6

Table 1
Thermal, chemical and physical properties of candidates for cermet fuel

	Cr	Mo	W	Si	Zr	ZrO_2	UO_2
Thermal conductivity ($W\,m^{-1}\,K^{-1}$)	90.3	138	178	148	22.7	4–6	3–8
Melting point (K)	1860	2620	3400	1410	1850	2720	2840
Heat capacity at R.T. ($J\,K^{-1}\,mol^{-1}$)	23.3*	23.8*	24.4*	20.0*	26*	57**	64**
Linear expansion coefficient at R.T. (10^{-6} K^{-1})	8.4	5.1	4.5	4.2	5.8	8.8	9.4
Density ($g\,cm^{-1}$)	7.19	10.22	19.3	2.33	6.51	5.8	10.9
Thermal neutron capture cross-section (10^{-24} cm^2)	3.1	2.5	19.2	0.13	0.185	0.2	8

To be compared with * $3R = 25\ J\,K^{-1}\,mol^{-1}$; ** $9R = 75\ J\,K^{-1}\,mol^{-1}$.

Although this result was calculated under the following simplifications, (1) the thermal conductivity of oxide was neglected, (2) the thermal conductivity was constant throughout the fuel, (3) the power distribution was constant in the fuel, it was possible to compare the temperature distributions among different fuels. Consequently, the maximum fuel center-line temperatures of cermet were estimated to be less than ≈1273 K.

For cermet fuels, it is essential to have direct contact between the oxide fuel and the metal matrix. Therefore, it is very important to investigate the compatibility between them at the fuel operating condition. In the present study, considering their neutron capture cross-sections, Zr and Si were selected as candidates for the metal matrix (see Table 1). So far, several types of cermet fuels have been developed and a compatibility study has been done for each cermet fuel system, e.g. Al–UO_2, Mo–UO_2 [6]. An idea of the liquid–metal-bonded gap for LWR fuels has been proposed and this may be considered to be a kind of cermet fuel system [7]. Although YSZ is the key material of the oxygen ion conductor as well as the host material of the nuclear fuel, the interaction between YSZ and metal has received little study of a chemical thermodynamic nature. In the present study, the reaction of YSZ with Zr, Si or Zircaloy-4 was investigated for a temperature range of 1073–1423 K for a maximum of 112 days.

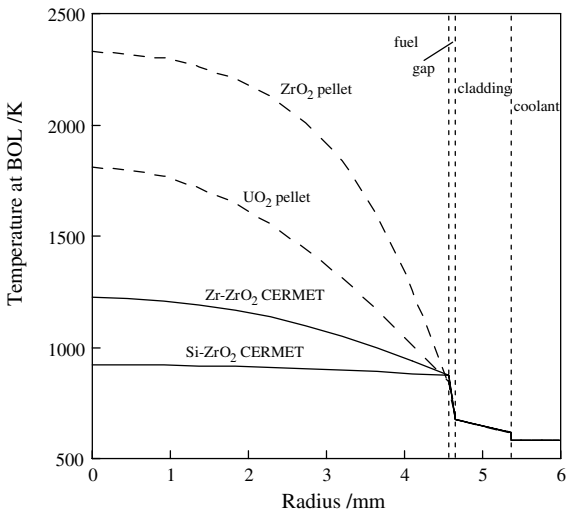

Fig. 1. Temperature distribution in cermet fuel at BOL (beginning of life). Linear heating rate = 40 $kW\,m^{-1}$; metal/oxide volume ratio of cermet fuel = 50/50; fuel-cladding gap temperature = 200 K.

2. Experimental

The zirconia specimens used in this experiment were fully stabilized $Y_yZr_{1-y}O_{2-y/2}$ $(y = 0.15)$. In order to confirm that this material had cubic structure, X-ray diffractometry (XRD) was performed. As a result, the diffraction pattern of only the cubic structure was measured, and the lattice parameter was estimated to be 5.14 Å. The YSZ specimens were prepared into the form of a disk, which had the geometry of 10 mm diameter and 1 mm thickness. Their surfaces were polished on abrasive papers and then subsequently finished by alumina buffing.

For the preparation of metal materials, Zr (99.7%), Si (99.99%) and Zircaloy-4 (ASTM chemical composition) were formed into samples which had the dimension of $10 \times 10 \times 1$ mm, $\varnothing 10 \times 1$ mm and $\varnothing 10 \times 1$ mm, respectively. For these metal materials, the surfaces were also polished mechanically as mentioned above.

The heated sample was the YSZ disk sandwiched between the metal samples, which were clamped between Mo plates. Each sample was put in a silica glass tube which was evacuated to a pressure of $\approx 10^{-3}$ Torr. The schematic view of the test sample for isothermal heating can be seen in Fig. 2. The heating temperature varied from 1073 to 1423 K. The samples were heated to the maximum in 112 days.

After isothermal heating, the sample was removed from the silica tube and was analyzed by an electron probe microanalyzer (Shimadzu EPMA-1600). For EPMA examinations, cross-sections of samples embedded in an acrylic resin were observed. The surfaces of the observed sections were mechanically polished with

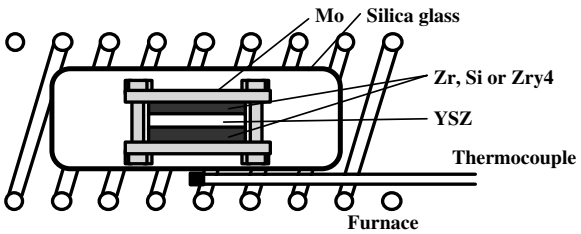

Fig. 2. Experimental set-up for isothermally heating. The heated sample was a YSZ disk sandwiched between metals such as Zr, Si and Zircaloy-4.

diamond paste and were then rinsed in an ultra-sonic bath. The surface of the observed section was covered with Au film to improve the electrical conductivity. Photographs taken by EPMA examinations were presented as back-scattering electron images (BEI) because it easily clarified the difference in distribution due to the average weight of elements. Furthermore, in order to measure the distribution of elements, characteristic X-rays of Lα–Zr, Lα–Y, Kα–O, Kα–Si and Lα–Sn were detected using analyzing crystals of ADP, PET, LS7A and PETs, respectively.

3. Results and discussion

3.1. Zr–YSZ and Zry4–YSZ

At a temperature less than 1273 K, interaction between Zr and YSZ was not observed. At high temperatures, $\geqslant$ 1273 K, reaction layers were observed between Zr and YSZ and internal changes of YSZ were also observed, especially for long term experiments. Fig. 3 shows the back-scattering electron images (BEI) and line analyses in the vicinity of the interface between Zr and YSZ for a sample heated to 1373 K for 5 d. The Zr layer strongly adhered to the surface of YSZ and the adherent layer fractured at a certain depth in the metal. Hereafter, the thickness of the adherent layer was defined as that of the reaction layer for Zr– and Zry4–YSZ samples. In terms of the chemical composition, the line analyses of EMPA showed that the oxygen content of the reaction layer was a little higher than that of the Zr matrix. It is known that zirconium easily absorbs oxygen and that the oxygen solubility in Zr is 30 at.%. Therefore, this α-phase of Zr that formed in the reaction layer had a high oxygen content and consumed the oxygen of the YSZ. In addition, every reaction layer observed at the interface between Zr and YSZ was peeled from the metal matrix. It may be related to mismatch of the thermal expansion. The thermal expansion $\Delta L \cdot L_0^{-1}$ of Zr was known to be 0.7% at 1373 K, and ≈1% for YSZ [8,9]. Therefore, at high temperature, the surfaces of the Zr

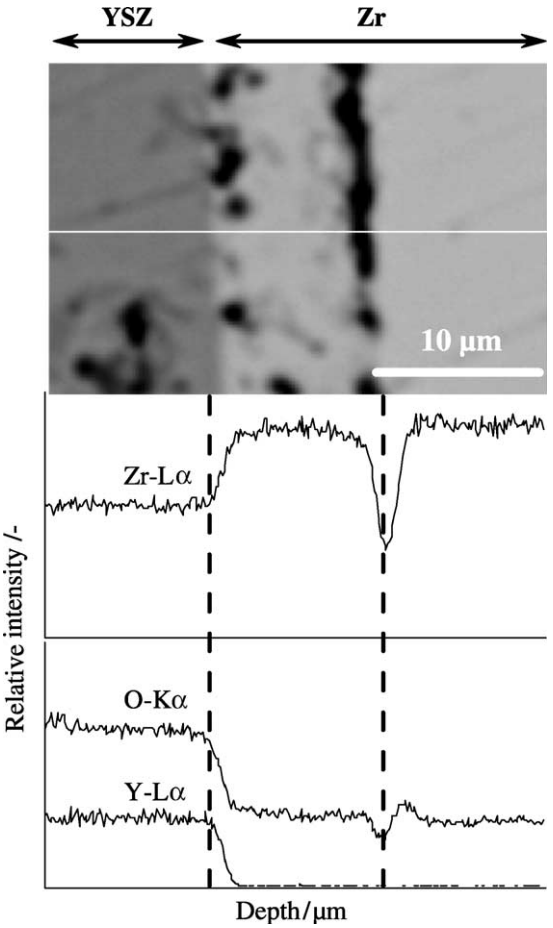

Fig. 3. Back-scattering electron image (BEI) and line analyses of the interface between Zr and YSZ. The sample was heated at 1373 K for 5 d. Line analyses were done along the white line shown in BEI.

and the YSZ were tightly pressed together so that the metallic reaction layer was probably peeled from its matrix in the cooling process due to the difference in thermal expansion.

The changes observed in the interior of the YSZ are shown in Fig. 4. In this figure, the BEIs taken from the cross-sections of samples heated at 1273 and 1373 K are shown. At the initial stage of heating, the white precipitates seen in the BEI emerged at the grain boundaries. The EPMA measurements clarified that these contained little oxygen and were like metal rather than oxide. These phenomena are related to both the oxygen affinity of coupled Zr and the oxygen diffusion property of YSZ. The YSZ is known to be an oxygen-ion conductor and the oxygen diffusion coefficient is larger at grain boundaries than within grains. Therefore the oxygen atoms existing around the grain boundaries moved into the coupled Zr at first. With increasing temperature and

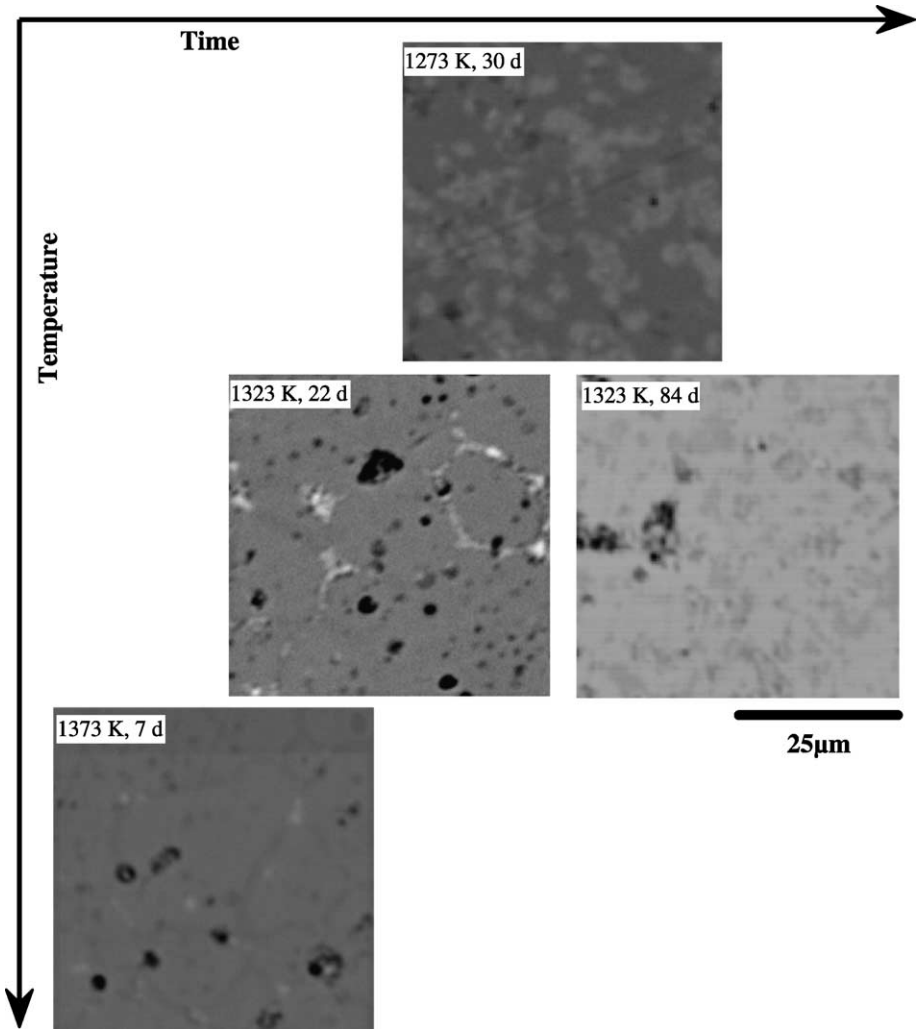

Fig. 4. Formation of metallic phases in the interior of YSZ coupled with Zr. These metallic phases were distributed uniformly in the YSZ.

heating time, each white precipitate extended its area and they were distributed uniformly in the YSZ.

In the Zry4–YSZ samples, neither the reaction layer between Zircaloy-4 and YSZ nor the metallic phases in YSZ could be found at $T \leqslant 1273$ K. Above a temperature of 1273 K, the reaction layers could be observed, and the metallic phases could also be observed after long periods of time. These changes observed in the Zry4–YSZ samples were similar to those of Zr–YSZ samples. Fig. 5 shows the BEI and line analyses at the vicinity of the interface between Zry4 and YSZ, and this sample was heated to 1323 K for 22 d. The condensation of tin, which is one of the alloy elements of Zircaloy-4, was observed. Such tin condensations were observed in almost all samples heated at $T > 1273$ K and occurred at the gap between the reaction layer and the Zircaloy-4 matrix. The content was ≈2–3 times of the 1.3 wt% of Sn initial content in Zircaloy-4. Such an amount of tin can be soluble in Zircaloy-4 (or Zr) in consideration of the Zr–Sn phase diagram [10]. The EPMA measurement, however, showed that tin was swept away in the reaction layer. It is difficult, so far, to understand clearly these results.

3.2. Si–YSZ

With heating temperatures lower than 1273 K, interactions between Si and YSZ are not observed. Above a temperature of 1273 K, a reaction layer is formed at the surface of the YSZ. Fig. 6 shows the BEI and line analyses at the vicinity of the interface between Si and YSZ. This sample was heated to 1373 K for 7 d. The

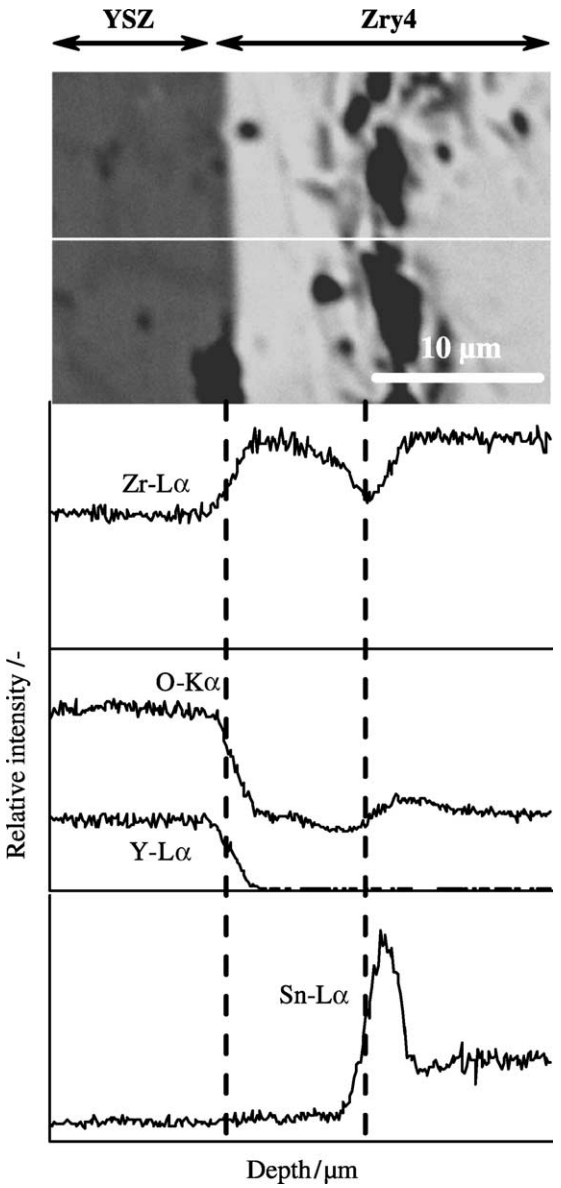

Fig. 5. BEI and line analyses of the interface between Zircaloy-4 and YSZ. The sample was heated at 1323 K for 22 d. Line analyses were done along the white line shown in BEI.

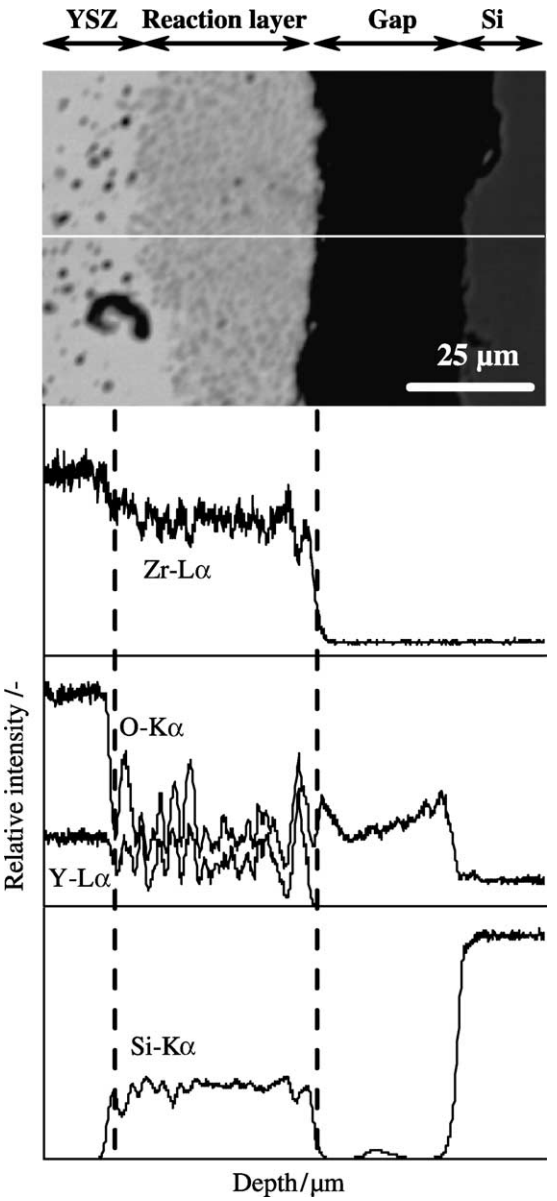

Fig. 6. BEI and line analyses of the interface between Si and YSZ. The sample was heated at 1373 K for 7 d. Line analyses were done along the white line shown in BEI.

reaction layer was characterized by two features. One is that the thickness of the reaction layer was much greater than those of Zr– and Zry4–YSZ samples, and another is that the reaction layer formed on the YSZ side. The line analyses clarified that Si combined preferentially with Zr, and that Y and O moved in the opposite direction to Zr. And two chemical phases, i.e. $Y_{0.11}Zr_{0.26}Si_{0.63}$ and $Y_{0.06}Zr_{0.11}Si_{0.33}O_{0.5}$, could be found in the reaction layer. The composition thus obtained had an error of roughly $\pm 10\%$ for each value due to the analyzed position or the experimental condition.

3.3. Kinetics of reaction layers

In Fig. 7, the thickness of reaction layer was plotted as a function of time for a sample heated to $T = 1373$ K. Fig. 8 shows the Arrhenius relationship between the reaction rate constant and the reciprocal of temperature. The rate constant was deduced under the assumption that the reaction layer grew parabolically with time. The reaction layers of Zr– and Zry4–YSZ samples had small growth rates. This was the reason the formation process

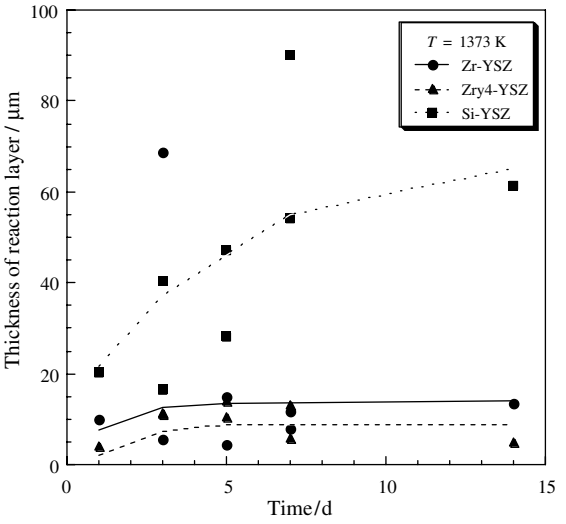

Fig. 7. Growth curve of reaction layer at a temperature of 1373 K.

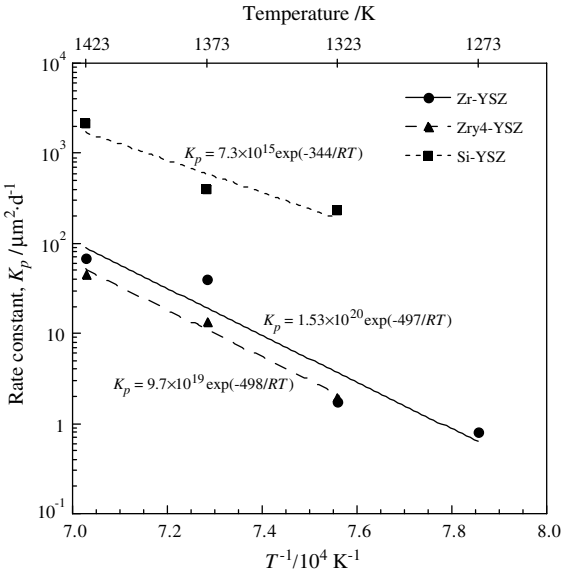

Fig. 8. Arrhenius relationship of reaction layer growth. The rate constant was calculated under the assumption that reaction layer growth obeyed the parabolic rate law. The activation energy thus obtained was expressed in unit of kJ mol^{-1}.

of reaction layers was not only relevant to chemical interaction, but also to the mechanical fracture. If the chemical interaction dominates the kinetics, the oxygen diffusion in Zr or Zircaloy-4 has to be considered. The oxygen diffusion coefficient in α-Zr was reviewed by Ritchie [11]. The oxygen diffusion pathway was estimated to be ≈2 mm in α-Zr at 1373 K for 14 d, and the value thus obtained was much larger than observed in this work (Fig. 7). In terms of the activation energy, the values of ≈500 kJ mol^{-1} obtained in the present study were larger than that of oxygen diffusion in α-Zr (229 kJ mol^{-1}). In addition, the oxygen supply was controlled by the equilibrium oxygen partial pressure of the Zr (or Zry4)–YSZ system [12]. The equilibrium oxygen partial pressure was estimated to be $P(O_2) = 4.4 \times 10^{-18}$ atm and at 1373 K for $Y_yZr_{1-y}O_{2-(y/2)} = Y_yZr_{1-y}O_{2+x-(y/2)} + (x/2)O_2(g)$ where $y = 0.148$. For the Zr–ZrO_2 system, the $P(O_2)$ was estimated to be 2.3×10^{-32} atm at 1373 K. In either case, the amount of supplied oxygen was very limited in terms of the oxygen partial pressure. Consequently, the oxygen was distributed evenly in Zr (or Zircaloy-4) at a concentration of less than the oxygen solubility limit. In the Zry4–YSZ samples, tin condensed in the gap between the reaction layer and Zircaloy-4 matrix. The correlation between the growth rate of the reaction layer and the chemical interaction was strong compared with the Zr–YSZ samples. However, from the aspect of chemical interaction only, the kinetics of reaction layer growth could not be understood. Therefore, as mentioned in Section 3.1, the difference in the mechanical property, e.g. thermal expansion, between metal and oxide might have an effect on the thickness of the reaction layer of Zr– and Zry4–YSZ samples.

On the other hand, the Si–YSZ samples showed a growth curve whose rate constant was relatively large. In addition, the thickness of reaction layer was increased with heating time. As shown in Fig. 6, in the reaction layer, cracks due to mismatch of thermal expansion could not be observed. Therefore, the chemical interaction determined the thickness of the reaction layer. Nevertheless, the reaction between Si and YSZ was a solid–solid or gas–solid reaction, the consideration of the reaction of YSZ with Si vapor under low oxygen partial pressure was helpful to understand the formation process of the reaction layer. The oxygen partial pressure in the Si–YSZ system might be less than the equilibrium one ($= \approx 6.9 \times 10^{-25}$ atm) between Si and SiO_2 at 1373 K because Si was not oxidized. Under such low oxygen partial pressures, Si and SiO vapor are the main chemical species. Consequently $(Zr,Y)Si_2$ may be formed in YSZ as a result of chemical thermodynamics equilibrium [13], and other chemical compounds containing oxygen atoms formed, since the zirconia was doped with 8 mol% Y_2O_3.

4. Conclusion

In the present study, the compatibility between yttria-stabilized zirconia and zirconium, silicon or Zircaloy-4 has been investigated at temperatures from 1073 to 1423 K. For the YSZ–Zr and –Zry4 systems, relatively thin reaction layers were observed at the interface

between YSZ and the metal at $T > \approx 1273$ K. The thickness of reaction layer, which was originally a part of the metal matrix, might be determined by both chemical interactions, e.g. oxygen diffusion, and mechanical interactions, e.g. mismatch of thermal expansion. For the YSZ–Zry4 samples, Sn condensation could be observed. In addition, the samples heated at high temperatures for long periods of time showed the occurrence of metallic phases in YSZ. On the other hand, in the YSZ–Si system, Si attacked YSZ at $T > 1273$ K so that the reaction layers formed on the YSZ side. The growth rate of the reaction layer of YSZ–Si samples was much larger than those of YSZ–Zr and YSZ–Zry4 samples. However, in terms of compatibility, the proposed systems in the present study was found to be suitable for utilization in pile because the maximum fuel center-line temperatures for cermet fuels and the temperature of the fuel cladding gap was estimated to be less than 1273 K.

Acknowledgements

This work was financially supported by the Japan Nuclear Cycle Development Institute. The authors gratefully acknowledge the continuous support by M. Kutsuwada, Department of Applied Quantum Physics and Nuclear Engineering, Kyushu University. The authors also wish to thank K. Wakasugi, Department of Materials Science and Engineering, for his help in EPMA measurements and Dr M. Watanabe, the Center of the Advanced Instrumental Analysis, for her help in XRD measurements.

References

[1] C. Degueldre, U. Kasemeyer, F. Botta, G. Ledergerber, Mat. Res. Soc. Symp. Proc. 412 (1995) 15.
[2] S. Raghavan, H. Wang, R.B. Dinwiddie, W.D. Porter, M.J. Mayo, Scr. Mater. 39 (1998) 1119.
[3] M.A. Pouchon, C. Degueldre, P. Tissot, Thermochim. Acta 323 (1998) 109.
[4] P.G. Klemens, M. Gell, Mater. Sci. Eng. A 245 (1998) 143.
[5] K. Idemitsu, PSI Technical Report TM-43-97-29, 1997.
[6] S. Nazaré, G. Ondracek, F. Thümmler, High Temp. High Press. 3 (1971) 615.
[7] Y.S. Kim, D.R. Olander, S.K. Yagnik, Nucl. Technol. 128 (1999) 300.
[8] Y.S. Touloukian, E.H. Buyco, Thermophysical properties of matter, vol. 12, Thermal expansion-metallic elements and alloys, Plenum, New York, 1970.
[9] S.P. Terblanche, J. Appl. Cryst. 22 (1989) 283.
[10] N. Dupin, I. Ansara, C. Servant, C. Toffolon, C. Lemaignan, J.C. Brachet, J. Nucl. Mater. 275 (1999) 287.
[11] I.G. Ritchie, A. Atrens, J. Nucl. Mater. 67 (1977) 254.
[12] J.H. Park, R.N. Blumenthal, J. Am. Ceram. Soc. 72 (1989) 1485.
[13] N. Bertolino, U.A. Tamburini, F. Maglia, G. Spinolo, Z.A. Munir, J. Alloys Comp. 288 (1999) 238.